AMERICAN SOCIETY FOR MICROBIOLOGY | mBio®

RESEARCH ARTICLE

Serine Deamination Is a New Acid Tolerance Mechanism Observed in Uropathogenic *Escherichia coli*

Michelle A. Wiebe,[a] John R. Brannon,[b] Bradley D. Steiner,[a]* Adebisi Bamidele,[a] Alexandra C. Schrimpe-Rutledge,[a,e] Simona G. Codreanu,[a,e] Stacy D. Sherrod,[a,e] John A. McLean,[a,e] Maria Hadjifrangiskou[b,c,d]

[a]Vanderbilt University, Nashville, Tennessee, USA
[b]Department of Pathology, Microbiology & Immunology, Vanderbilt University Medical Center, Nashville, Tennessee, USA
[c]Department of Urology, Vanderbilt University Medical Center, Nashville, Tennessee, USA
[d]Institute for Infection, Immunology & Inflammation, Vanderbilt University Medical Center, Nashville, Tennessee, USA
[e]Center for Innovative Technologies, Department of Chemistry, Vanderbilt University, Nashville, Tennessee, USA

ABSTRACT *Escherichia coli* associates with humans early in life and can occupy several body niches either as a commensal in the gut and vagina, or as a pathogen in the urinary tract. As such, *E. coli* has an arsenal of acid response mechanisms that allow it to withstand the different levels of acid stress encountered within and outside the host. Here, we report the discovery of an additional acid response mechanism that involves the deamination of L-serine to pyruvate by the conserved L-serine deaminases SdaA and SdaB. L-serine is the first amino acid to be imported in *E. coli* during growth in laboratory media. However, there remains a lack in knowledge as to how L-serine is utilized. Using a uropathogenic strain of *E. coli*, UTI89, we show that in acidified media, L-serine is brought into the cell via the SdaC transporter. We further demonstrate that deletion of the L-serine deaminases SdaA and SdaB renders *E. coli* susceptible to acid stress, similar to other acid stress deletion mutants. The pyruvate produced by L-serine deamination activates the pyruvate sensor BtsS, which in concert with the noncognate response regulator YpdB upregulates the putative transporter YhjX. Based on these observations, we propose that L-serine deamination constitutes another acid response mechanism in *E. coli*.

IMPORTANCE The observation that L-serine uptake occurs as *E. coli* cultures grow is well established, yet the benefit *E. coli* garners from this uptake remains unclear. Here, we report a novel acid tolerance mechanism where L-serine is deaminated to pyruvate and ammonia, promoting survival of *E. coli* under acidic conditions. This study is important as it provides evidence of the use of L-serine as an acid response strategy, not previously reported for *E. coli*.

KEYWORDS *Escherichia coli*, acid stress, bacterial stress response, metabolomics, serine

Acid stress is a substantial challenge to bacterial life. Acidic conditions can damage the bacterial cell envelope, rendering membrane-embedded proteins and the proton motive force established across the membrane dysfunctional or nonfunctional (1). Acidic conditions in the bacterial cell interior disturb vital physiological processes, such as enzymatic activity, protein folding, membrane, and DNA maintenance, all of which are needed for cellular function and can cause bacterial death. As a result, bacteria are equipped to withstand acidic conditions. One of the model bacterial organisms, *Escherichia coli*, occupies numerous environmental and host niches and encounters a range of acidic conditions in a niche-dependent manner. For example, all *E. coli* harbored in the gut are thought to be acquired via ingestion (2), indicating that *E. coli* must be able to survive the low pH of the stomach, which ranges from pH 1.5 to 3.5 (3–5). It is therefore not surprising that five acid resistance (AR) mechanisms, termed AR1 to AR5, have been identified in *E. coli*, all of which have been shown to be active in the gut (6, 7).

Invited Editor Tracy Lyn Raivio, University of Alberta

Editor Scott J. Hultgren, Washington University School of Medicine

Address correspondence to Maria Hadjifrangiskou, maria.hadjifrangiskou@vumc.org.

*Present address: Bradley D. Steiner, Florida State University College of Medicine, Tallahassee, Florida, USA.

The authors declare no conflict of interest.

Received 25 October 2022
Accepted 9 November 2022
Published 5 December 2022

The most well characterized AR mechanisms, AR2-5, depend on the import and subsequent decarboxylation of specific amino acids. The decarboxylation reaction consumes one proton, thereby increasing the cytoplasmic pH. AR2, which has been shown to be the most effective AR mechanism in *E. coli*, involves the deamination of glutamine to glutamate, which is then decarboxylated to form γ-amino butyric acid (GABA) (3, 8–10). AR3 involves the decarboxylation of arginine to produce agmatine, while AR4 leads to decarboxylation of lysine to produce cadaverine. Finally, ornithine decarboxylation to putrescine is the basis of AR5 (10). The AR1 mechanism of action is not well understood.

While decarboxylation of amino acids appears to be the primary means of acid resistance in *E. coli*, there is evidence that deamination of amino acids can also serve to increase the intracellular pH. This is evident in AR2, where glutamine deamination not only provides the glutamate that is then decarboxylated (AR2_Q) (11, 12) but also produces ammonia which consumes a proton and diffuses out of the cell as ammonium (11, 13). Here, we demonstrate that the deamination of L-serine is an additional acid response mechanism in *E. coli*.

Notably, L-serine is the first amino acid consumed by *E. coli* when grown in complex media (14). Under aerobic conditions, it is known that L-serine is deaminated by SdaA and SdaB to produce pyruvate and ammonia (15). However, to date no metabolic role for serine deamination in *E. coli* has been described (16), as most of the pyruvate derived carbon is subsequently excreted from the cell (14). In *Klebsiella aerogenes* and *Streptococcus pyogenes* serine deamination has been shown to be important for regulating nitrogen balance and maintaining extracellular pH (17, 18), but the full import of serine deamination in these pathogens remains unclear.

Uropathogenic *E. coli* (UPEC) is an extraintestinal pathotype of *E. coli*, responsible for over 75% of reported urinary tract infections (19). UPEC strains have developed strategies to persist for years in the host (20–22), colonizing the gut, the vaginal space, and the bladder in asymptomatic reservoirs for long periods of time (23). UPEC has been reported to persist within the acidic environment of the vagina (pH 3.8 to 5) (24, 25) before ascending to and colonizing the urinary tract (pH 5.5 to 7) (4, 5). No studies have elucidated the mechanisms of acid tolerance in UPEC. In this work, we demonstrate that L-serine deamination is a previously unrecognized acid tolerance mechanism in UPEC. We show that under acidic conditions, serine is transported into the cell by the SdaC transporter and deaminated by the L-serine deaminases SdaA and SdaB, a process that imparts *E. coli* with protection from acid.

RESULTS

***YhjX* is upregulated in response to low pH in a manner that depends on the noncognate two-component system BtsS and YpdB.** Previous work indicated that L-serine induces the activation of the BtsS pyruvate sensor kinase (26), presumably due to production of pyruvate via SdaA/B mediated L-serine deamination. BtsS has been shown to induce the upregulation of the uncharacterized gene *yhjX*, in concert with a noncognate response regulator partner, YpdB (27). Interestingly, natural induction of *yhjX* has been previously reported by the Jung group to occur in *E coli* culture during midlogarithmic growth phase (28), when bacterial cell density is high and nutrient depletion of LB begins to occur. Moreover, previous studies have shown that *yhjX* is among the genes upregulated in response to acidic pH in K-12 *E. coli* (29). To confirm that these previous observations hold true in UPEC, we first assessed induction of *yhjX* in cystitis strain UTI89 (20). UTI89 is a sequence type ST95 strain, isolated from a patient with cystitis (20). UTI89 is an O18:K1:H7 serotype, typical of UPEC strains and its genome has been sequenced (20, 30). To monitor whether *yhjX* induction is indeed acid-responsive in UPEC, we used a previously constructed strain UTI89/P*yhjX*::lux (27) that harbors a plasmid containing the *yhjX* promoter fused to the *luxCDABE* operon (28). Luminescence and bacterial growth were monitored over time in unbuffered lysogeny broth (LB) with shaking. Cultures inoculated at near-neutral pH 7.4 to 7.6 (Fig. 1c, right y-axis) showed a peak in *yhjX* promoter activity at 180 min, coincident with late logarithmic phase of growth (Fig. 1b, Fig. S1, Data set S1). Addition of increasing concentrations of HCl to the media led to an increase in *yhjX* promoter activity that was proportional to the drop in pH (Fig. 1b and Data set S1). The addition of HCl under the conditions tested did not affect bacterial

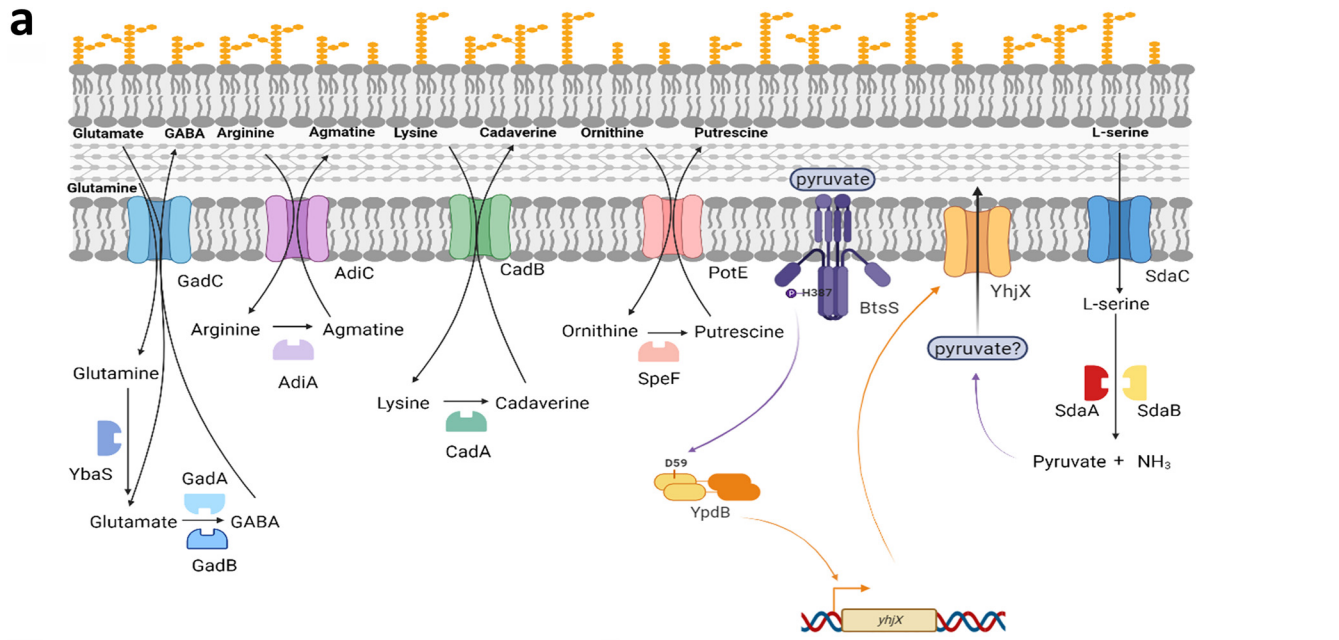

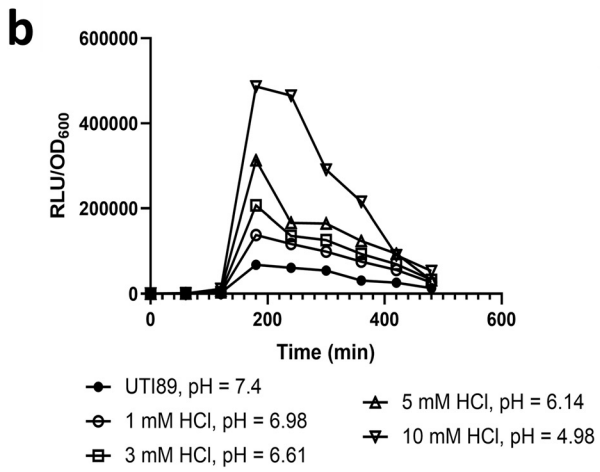

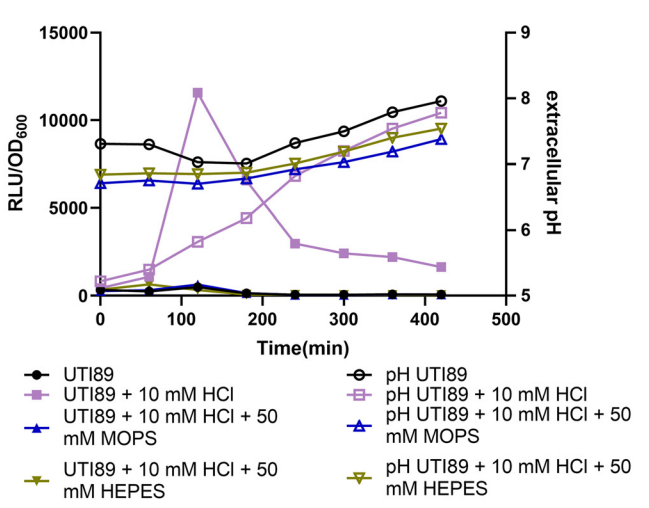

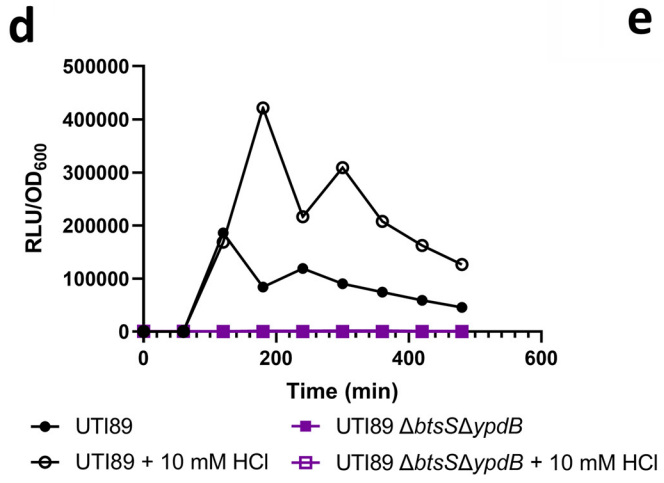

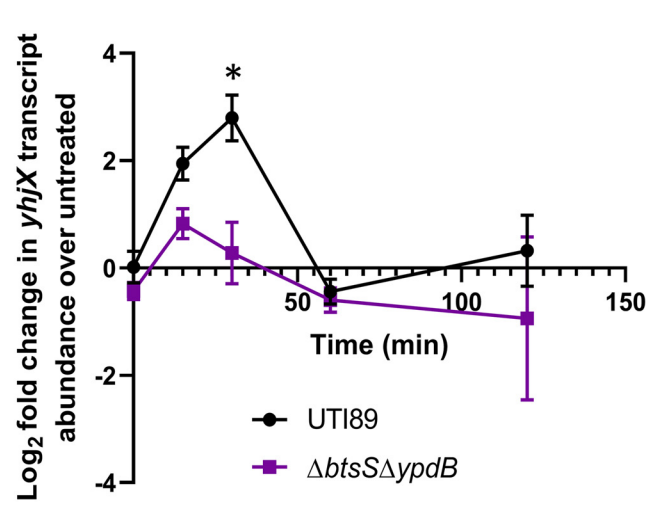

FIG 1 *yhjX* is upregulated in response to low pH in a manner that depends on the noncognate two-component system BtsS and YpdB. (a) Cartoon depicts currently known acid tolerance mechanisms in *E. coli*. Also depicted is our proposed novel acid tolerance mechanism that depends on L-SERINE import and

(Continued on next page)

growth (Fig. S1). Addition of buffer—either MOPS or HEPES—to the acidified culture media restored neutral pH and suppressed *yhjX* promoter activity to levels observed when grown in LB with pH 7.4 (Fig. 1c and Data set S1). These results indicate that *yhjX* is indeed an acid-induced target in UPEC and corroborate previous observations in K-12 strains of *E. coli*.

The *yhjX* gene encodes a putative pyruvate transporter of the major facilitator superfamily that has not yet been shown to import or export pyruvate (28, 31). Studies have shown that pyruvate increases in the extracellular milieu as the bacterial culture reaches late exponential growth (28), and that this pyruvate is directly sensed by the BtsS histidine kinase, leading to subsequent upregulation of *yhjX* via the action of the YpdB response regulator (27). To determine whether acid-mediated induction of *yhjX* is dependent on BtsS and YpdB, a mutant lacking both *btsS* and *ypdB* (Δ*btsS*Δ*ypdB* [27]) was tested via our luminescence reporter assay in acidic and neutral conditions. These experiments showed no induction of *yhjX* in the Δ*btsS*Δ*ypdB* strain, regardless of pH in the culture media (Fig. 1d and Data set S1). To validate these findings, *yhjX* steady-state transcript over time was also monitored by RT-qPCR and TaqMan based chemistry in acidified and nonacidified cultures of wild-type UTI89 and the isogenic Δ*btsS*Δ*ypdB* mutant. Transcript abundance of *yhjX* was compared between acid stimulated and unstimulated growth conditions and normalized to the *gyrB* housekeeping gene. These analyses revealed a characteristic transcription surge (32) for *yhjX* in acidified wild-type UTI89 cultures, which was not apparent in the isogenic Δ*btsS*Δ*ypdB* (Fig. 1e). To further confirm that *yhjX* is induced by low pH and not just HCl, we utilized the luminescent reporter to monitor *yhjX* induction in UTI89 and Δ*btsS*Δ*ypdB* in the presence of lactic acid, acetic acid, and pyruvic acid (Fig. S2, Data set S1). All organic acids tested resulted in strong *yhjX* induction in UTI89. However, the Δ*btsS*Δ*ypdB* strain did not induce *yhjX* under any of these acidic conditions (Fig. S2 and Data set S1). Notably, addition of HCl, or acetic acid occasionally leads to two peaks in luminescence (Fig. 1d, Fig. S2) in wild-type UTI89, indicative of two activation surges for *yhjX* transcription. This phenomenon is likely connected to BtsS signaling, but why it occurs only in response to HCl or acetic acid is unknown. Together, these data confirm that *yhjX* is induced in low-pH growth conditions and that this induction depends on the presence of BtsS and YpdB.

Induction of BtsS-YpdB in response to acid results from pyruvate produced during L-serine deamination. Previous work demonstrated that BtsS signaling is affected by L-serine levels in the growth medium (33). These studies postulated that L-serine, which is the first amino acid to be consumed by *E. coli* during growth in laboratory media (14), is converted to pyruvate by the L-serine deaminases SdaA and SdaB and could then presumably exported by YhjX to serve as a positive feedback signal for BtsS (15, 34, 35) and (Fig. 1a). Given that the deamination of L-serine also produces ammonia, which can raise intracellular pH (Fig. 1a), we asked whether the mechanism of acid stress alleviation observed in our studies depends on the import and deamination of L-serine. To test this hypothesis, we first created a series of mutants lacking the SdaC transporter (Δ*sdaC*), the SdaA or SdaB deaminases (ΔsdaA, Δ*sdaB*) or both deaminases (Δ*sdaA*Δ*sdaB*). The induction of *yhjX* in these mutants was tested via luciferase reporter assays either in media in which exogenous L-serine was added (Fig. 2a and Data set S1), or in media acidified with HCl (Fig. 2b and Data set 2). Addition of L-serine did not induce *yhjX* promoter activity in any of the *sda* mutants (Fig. 2a and Data set S1). Addition of acid to the media led to decreased *yhjX* induction compared to wild-type UTI89 in all the single mutants tested and led to no *yhjX* induction in the Δ*sdaA*Δ*sdaB* strain (Fig. 2b, Data set S1). Given that pyruvate is the known ligand of the BtsS sensor, our data suggest that *in vivo* it is the deamination of L-serine into pyruvate that

FIG 1 Legend (Continued)
deamination. The signaling system BtsS-YpdB and its downstream target *yhjX* that codes for a putative transporter, are also induced during acid stress. Cartoon was created using BioRender.com. (b–c) Graphs depict relative luminescence units (RLU) normalized to growth (OD_{600}) over time, of UPEC strain UTI89 harboring the P*yhjX-lux* reporter in increasing concentration of HCl (b) or during growth in LB buffered to a pH of 7 with either 50 mM MOPS or 50 mM HEPES (c). (d) Luciferase reporter assay of UPEC strain UTI89 the isogenic Δ*btsS*Δ*ypdB* strain grown in the presence (initial pH of 5.0) or absence (initial pH of 7.4) of HCl. Graphs are representative of 3 independent biological repeats. (e) RT-qPCR analysis of *yhjX* transcript abundance after acid stimulation (pH of 5) in wild-type UTI89 (black) and Δ*btsS*Δ*ypdB* (purple) strains. Relative fold change was determined by the $\Delta\Delta C_T$ method, where transcript abundances were normalized to *gyrB* housekeeping gene transcripts. *, $P = 0.0165$ calculated by two-way ANOVA with Sidak's multiple-comparison test. Error bars indicate SEM of three biological replicates.

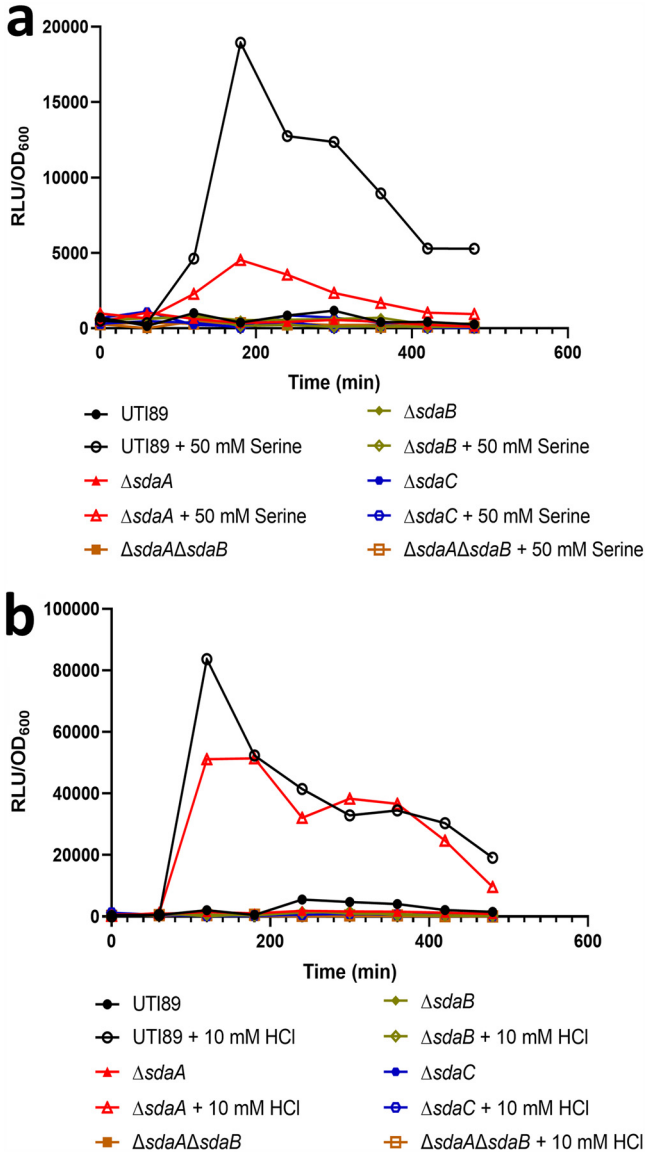

FIG 2 Induction of BtsS-YpdB in response to acid results from pyruvate produced during L-SERINE deamination. Graphs depict luciferase reporter assay performed over time of strains harboring the *yhjX* promoter reporter during growth in media supplemented with 50 mM serine (a) or 10 mM HCl (b). Deletion of serine import (*sdaC*, blue) or deamination genes (*sdaA*, red; *sdaB*, gold) diminishes *yhjX* promoter activity. Results are representative of 3 biological repeats.

actually leads to *yhjX* being induced. As further evidence that it is the generation of pyruvate driving *yhjX* induction, sodium pyruvate was added to the media of the Δ*sdaA*Δ*sdaB* strain, which caused—as expected—*yhjX* induction (Fig. S3 and Data set S1).

L-serine deamination is a mechanism that protects *E. coli* from acid stress. If L-serine deamination is a component of the *E. coli* acid response, we reasoned that the mutant lacking the SdaA/B enzymes would display a survival defect in acidic conditions. We first determined the acid tolerance profile of UTI89, given that we have not previously tested this strain for acid sensitivity. To do this, we subcultured UTI89 in fresh, unbuffered LB (pH 7.4) for 3 h then adjusted the culture pH to 7, 6, 5, 4, 3, or 2 using HCl. We then assessed survival of UTI89 after 30 min or 2 h of exposure. As expected, wild-type UPEC survival did not get substantially affected during 30 min incubation at pH 3 but decreased by 2 logs during the 2 h of incubation (Fig. 3a and S4a). Incubation at pH 2 for 30 min and 2 h both had substantial impact on UPEC growth (Figure 3a and Fig. S4a). To compare the effects of *sda* deletion on acid tolerance, we picked 30-minute incubation at pH 3, since these conditions do

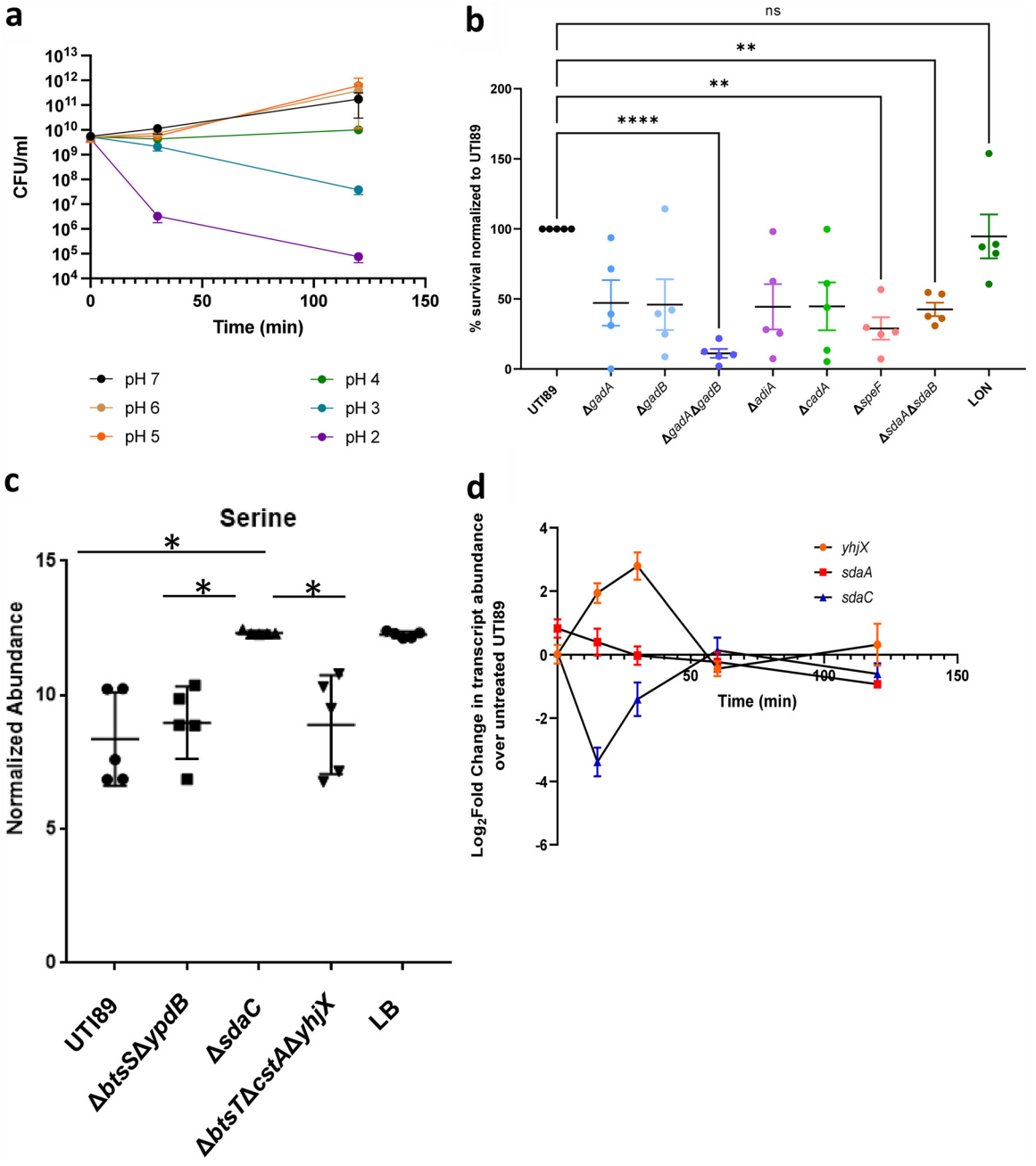

FIG 3 L-serine deamination is another acid resistance mechanism in *E. coli*. (a) CFU/mL of UTI89 grown in LB adjusted to the indicated pHs with HCl ($n = 4$ biological replicates). (b) Graph depicts survival in acidic conditions, compared to the wild-type strain, of mutants deleted for decarboxylases or serine deaminases. For these assays, cultures were incubated for 3 h, at which point an aliquot was collected for CFU enumeration before acid treatment. The remaining culture was treated with HCl to adjust the pH to three. Samples were incubated for an additional 30 min, after which they were plated for CFU. Percent survival in acid is calculated as the number of CFU in acid treatment, compared to untreated input control. Statistical analysis was performed by 1-way ANOVA with *post hoc* Dunnett's multiple comparisons correction test (**, $P < 0.005$; ****, $P < 0.0001$). Error bars indicate SEM of 5 biological replicates. (c) UTI89, Δ*btsS*Δ*ypdB*, and Δ*sdaC* were grown until cultures reached an $OD_{600} = 0.5$, then 1 M HCl was added to the culture to a final concentration of 10 mM (pH = 5). Cultures were incubated for another 15 min, then 1 mL of culture was collected. Cells were pelleted and supernatant was flash frozen and stored at −80°C prior to sample preparation. Following MS sample preparation, extracellular serine abundance was detected by LC-MS. (d) qPCR analysis of *yhjX* (orange), *sdaA* (red), and *sdaC* (blue) transcript abundance after acid stimulation in wild-type UTI89. The relative fold change was determined by the $\Delta\Delta C_T$ method where transcript abundances were normalized to *gyrB* housekeeping gene transcripts. Error bars indicate SEM of three biological replicates (*, $P < 0.005$, ANOVA).

not significantly impact survival of wild-type UTI89. Under the selected conditions, we observed the Δ*sdaA*Δ*sdaB* strain exhibiting the most pronounced acid survival defect compared to any of the single Δ*sdaA*, Δ*sdaB,* or Δ*sdaC* mutants (Fig. S5). The acid susceptibility profile of Δ*sdaA*Δ*sdaB* is similar to known acid resistance mutants cultured under the same conditions (Fig. 3b). The survival defect of Δ*sdaA*Δ*sdaB* was also observed when the strain was incubated for 2 h in pH 3, compared to wild-type UTI89 or an isogenic Δ*gadA*Δ*gadB* strain (Fig. S4b; pH 3 data). Intriguingly, when we tested Δ*sdaA*Δ*sdaB* and Δ*gadA*Δ*gadB* in pH 2 for 30 min, we observed a similar decline in CFU that was not statistically different from wild-type UTI89 (Figure S4c; pH 2, 30-minute data). These observations indicate a different susceptibility profile for UPEC, compared to commensal *E. coli* (36, 37) and demonstrate that L-serine deamination becomes an important acid tolerance mechanism for UPEC.

To determine if serine is imported by *E. coli* in response to a drop in pH, cell culture supernatants were then analyzed for relative serine abundance by LC-MS and compared to acidified media alone as a control. Mass spectrometric measurements of serine in media alone demonstrated that baseline serine abundance level can be detected with this method (Fig. 3c and Data set S2). Measurements of serine in acidified media revealed a significant reduction in extracellular serine abundance in the supernatant fractions of WT UTI89, but not the Δ*sdaC* mutant (Fig. 3c and Data set S2). These data indicate that serine is imported—in an SdaC-dependent manner—into the bacterial cell in response to acid stress.

Extracellular serine levels also drop in the Δ*btsS*Δ*ypdB* mutant under acidic conditions (Fig. 3c and Data set S2). This observation is consistent with the notion that L-serine is imported independent of BtsS-YpdB signaling. Subsequent qPCR showed that in the wild-type strain *sdaA* transcript abundance does not significantly change in response to acid stress (Fig. 3d), in sharp contrast to *yhjX* that displays an activation surge (Fig. 3d). These data indicate that *sdaA* transcription is not acid inducible. Interestingly, *sdaBC* transcript abundance sharply drops at 15 min post addition of acid to the media, displaying a fold change that is the opposite of *yhjX* (Fig. 3d). Maurer et al., previously reported sdaB and sdaC as "acid-low" transcripts (37). Our data indicated drop in transcript shortly after addition of acid and coincident to the time that L-SERINE is brought into the cell (Fig. 3b). This could indicate that acidic conditions lead to downregulation of *sdaBC* via an unknown regulator, or that production of pyruvate or ammonia by L-serine deamination has a negative impact on *sdaBC* transcription.

YhjX is induced in response to pyruvate detection by the BtsS sensor histidine kinase (33). Given that L-serine deamination leads to the production of pyruvate, which is the known ligand for BtsS (33), we hypothesized that SdaA/SdaB-mediated L-serine deamination increases intracellular pyruvate levels that could then be exported via YhjX, if the function of YhjX is to transport pyruvate (Fig. 4a). To determine if extracellular pyruvate abundance changes in response to acid treatment, we measured pyruvate levels in the extracellular milieu over time, following acidification of the culture media, in the same samples used for the serine measurements in Fig. 3c. Cell culture supernatants were analyzed for changes in pyruvate abundance using Pyruvate Assay kits (MAK071-1KT, Sigma-Aldrich) and fold change compared to non-treated controls was determined. In wild-type UTI89, an increase in extracellular pyruvate is observed at 15 min following acidification, compared to the untreated isogenic control (Fig. 4b, Data set S3). Following this pyruvate surge, pyruvate levels are not significantly higher between treated and untreated UTI89 cells at 60 and 180 minutes post acidification. In the mutant lacking the SdaC transporter, extracellular levels are significantly lower than those of wild-type UTI89 at 15 min post acidification, but still increase, suggesting that pyruvate is exported from the cell even when L-serine import is disrupted. In sharp contrast, the supernatant fractions of the Δ*btsS*Δ*ypdB* mutant, which as demonstrated in Fig. 1d, has no observable *yhjX* promoter activity (Fig. 4b), show no increase in extracellular pyruvate levels at 15 min following acidification. Instead, we observe an increase in extracellular pyruvate at 60 min post acidification for Δ*btsS*Δ*ypdB*. These data suggest that YhjX may indeed export pyruvate, although additional studies are needed to prove this biochemically. Our data also indicate that in the absence of YhjX, other transporters can presumably fulfill the function of pyruvate export, since extracellular pyruvate levels do increase at a later time point in the acid-treated Δ*btsS*Δ*ypdB* strain.

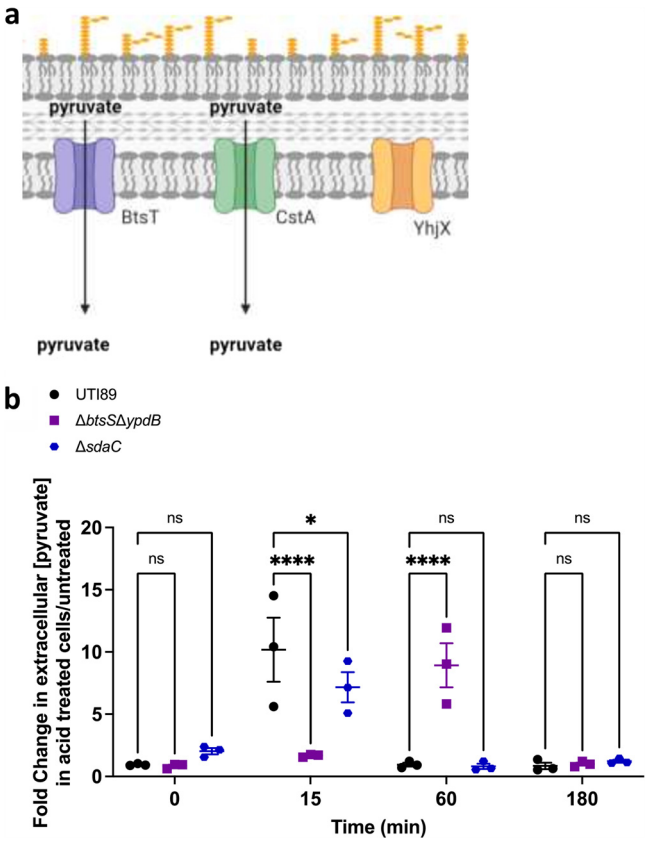

FIG 4 (a) Cartoon depicts currently known pyruvate transporters (BtsT and CstA) and a putative pyruvate transporter (YhjX) in *E. coli*. Created with BioRender.com. (b) UTI89, Δ*btsS*Δ*ypdB*, and Δ*sdaC* strains were grown until cultures reached an OD_{600} = 0.5, then split so that 1 M HCl was added to half of the culture while the other half continued to grow in LB alone. Supernatant was collected after 0, 15, 60, and 180 min. Pyruvate concentration in the supernatant was quantified for all time points. Fold change in pyruvate concentration in the acid treated samples over the unstimulated samples is graphed. Error bars indicate SEM of 3 biological replicates (****, $P < 0.001$; *, $P < 0.05$).

In conclusion, our data demonstrate that the import and deamination of L-serine provides protection from acid stress to uropathogenic *E. coli,* and we provide circumstantial evidence for export of pyruvate via YhjX under acidic conditions.

DISCUSSION

In this work, we show that L-serine deamination serves as an additional acid response mechanism in *E. coli*. Serine is the first amino acid consumed by *E. coli* when grown in complex media, despite its toxicity at higher concentrations (14). L-serine can be deaminated by the SdaA and SdaB enzymes to yield pyruvate and ammonia. *E coli* encodes multiple serine deaminase genes that function under a variety of environmental conditions (38). For instance, while both *sdaA* and *sdaB* are expressed under aerobic conditions, *sdaA* is expressed in nutrient limited minimal media, and in contrast, *sdaB* is expressed in the nutrient rich LB (16, 35, 39). The redundancy of these enzymes indicates that the deamination of serine is important for these bacteria. In this paper, we propose that L-SERINE import into *E. coli* serves as an acid tolerance mechanism through the production of ammonia and pyruvate. Maurer et al. profiled gene expression in K-12 *E. coli* in response to pH changes. Their work showed that serine deaminases were upregulated in basic conditions compared to acidic conditions (37). This is reflected in our qPCR data (Fig. 3d), where we show that *sdaC* is downregulated shortly after acidification. However, we see that sustained growth in acidic media led to an increase in *sdaC* transcript abundance over time (Fig. 3d). It is possible that acidic conditions lead to downregulation of *sdaBC* via an unknown

regulator, or that production of pyruvate or ammonia by L-serine deamination exerts negative feedback on *sdaBC* transcription.

Various bacteria are known to use ammonia to neutralize their intracellular pH, including *E. coli* (11, 40, 41). We postulate that the ammonia produced via L-serine deamination functions as a base which increases the cytoplasmic pH of *E. coli* when under acid stress. A similar role has been reported for glutamine (AR2_Q) in *E. coli* (11, 13). Deletion of the serine deaminase genes, *sdaA* and *sdaB*, results in a significant decrease in cell survival in acidic conditions compared to the wild-type strain. This decrease in cell survival is comparable to that observed in other AR mutants of *E. coli*. All together, these data suggest that L-serine deamination serves as a previously uncharacterized acid tolerance mechanism in *E. coli*. Loss of serine deaminase activity was previously shown to result in changes to cell shape due to interference with cell wall synthesis (16, 38). These serine deaminase mutants exhibit increased filamentation. In the context of UTI, filamentous UPEC are deficient in invading bladder cells, forming secondary intracellular bacterial communities, and in establishing quiescent intracellular reservoirs (42, 43). Thus, loss of serine deamination could detrimentally affect the ability of UPEC to form reservoirs in addition to its ability to tolerate low pH. Evolution of mechanisms that utilize various amino acids for tolerating acid stress would allow bacteria to seamlessly adapt to different host niches with differing resource availabilities during the infection process.

It has been shown that up to 51% of serine flux is directed to the production of pyruvate (14), which can presumably be shunted into the TCA cycle for energy production. Here, we demonstrate a connection between serine deamination and the pyruvate responsive cross regulating two-component system, BtsS-YpdB. BtsS-YpdB activation occurs in response to increased pyruvate and leads to the upregulation of *yhjX* transcription. Loss of L-serine deaminases result in ablation of *yhjX* promoter induction in response to serine, indicating that pyruvate produced via serine deamination induces activation of the BtsS-YpdB system. Our metabolomics analyses demonstrate that extracellular serine levels drop in the Δ*btsS*Δ*ypdB* mutant under acidic conditions indicating that BtsS-YpdB activation occurs after L-SERINE is imported. In this work we also show that *yhjX* is also induced by the BtsS-YpdB system in response to acidic pH (Fig. 1b–d). Although this activation in response to low pH was dose dependent, considering the data that suggests *yhjX* is induced through serine deamination and that pyruvate is a known ligand for BtsS, *yhjX* activation in response to low pH appears to be a response to the pyruvate produced by serine deaminases. The function of YhjX remains elusive. We, and others, have hypothesized that YhjX could serve as a pyruvate transporter. Here, we provide preliminary evidence that YhjX may function as a pyruvate transporter, but it is not necessary for the L-serine mediated acid response, as extracellular pyruvate levels do increase – albeit in a delayed fashion – in the Δ*btsS*Δ*ypdB* strain (Fig. 4b).

In summary we show that in acidified media, cells import L-SERINE from the growth media via the SdaC transporter and deaminate it via the action of SdaA and SdaB. Deletion of both deaminase genes renders *E. coli* susceptible to acid stress similarly to known AR system deletion mutants. We therefore propose that the importation and deamination of serine represents a previously uncharacterized acid response mechanism in *E. coli*.

MATERIALS AND METHODS

Bacterial strains and growth conditions. All studies were performed in the well characterized UPEC cystitis isolate UTI89 (20) and derived isogenic deletion mutants. UTI89 is of the sequence type ST95 and is serotyped as O18:K1:H7 (20). For all analyses, strains were propagated from a single colony in unbuffered lysogeny broth (LB) (Fisher Scientific), at pH 7.4. Inoculated strains were grown overnight at 37°C with shaking unless otherwise noted. Strains containing the luciferase reporter plasmid were grown in LB + 50 μg/mL gentamicin at 37°C, 220 rpm overnight. The pH at the beginning of the culture (pH 7.4) and end of the culturing (pH 8.56) was measured using Thermo Scientific Orion Star A211 pH meter with an Orion Green pH Combination Electrode. Specific growth conditions for reporter and survival assays are described in the relevant sections below. Gene deletions were created using the λ-red recombinase system (44). The Δ*btsS*Δ*ypdB* and Δ*yhjX* mutant strains were created in previous studies (27). The *yhjX::lux* reporter, which was previously constructed (28), was introduced into each strain via electroporation and validated by PCR.

A complete list of strains, primers, and plasmids used for in this study can be found in Tables S1 and S2.

Luciferase reporter assay. Overnight cultures were spun at 3220 × *g* for 10 min. Pellets were resuspended in 5 mL 1× PBS and repelleted. Pellets were resuspended in 5 mL 1× PBS and normalized to a starting OD_{600} = 0.05 in 1 mL of the indicated media (LB, LB + 10 mM HCl, or LB + 50 mM MOPS or HEPES buffer + 10 mM HCl). Each suspension was used to seed black, clear bottomed 96-well plates at 200 μL per

well from and grown at 37°C with shaking. OD_{600} and luciferase readings were taken every hour for 8 h using a Molecular Devices SpectraMax i3 plate reader. At least 3 biological replicates were assayed.

Acid tolerance assays. Acid tolerance assays were performed as follows: Bacteria were grown overnight as described above and diluted 1:100 in 5 mL of fresh, unbuffered LB at pH 7.4. Cultures were incubated at 37°C with shaking. When strains reached mid exponential growth phase (OD_{600} of ~3.0 at 3 h), 1 mL of the culture was centrifuged at 16,000 × *g* for 5 min, washed in 1× PBS, serially diluted and spot-plated for CFU to determine CFU prior to acid exposure (Input sample). The pH of the remaining 4-mL culture was adjusted to a pH of 3 using 5 M HCl, and acidified cultures were incubated at 37°C, with shaking for 30 min. Following incubation, 1 mL of the acidified sample was centrifuged, washed in PBS, and plated for CFU. Percent survival was calculated by dividing the CFU/mL after acid stress by the CFU/mL of the input sample. Statistical analysis was performed by 1-way ANOVA with *post hoc* Dunnett's multiple comparisons correction test.

RNA extraction and RT-qPCR. Growth conditions for RNA sample collection. To collect samples for transcriptional analysis, strains were grown aerobically in LB to an OD_{600} = 0.5 and then split into two conditions: continued growth in LB alone, or in LB in which HCl was added to a final concentration of 10 mM. Samples were taken for RNA extraction at time = 0, 15, 30, 60, and 120 min after splitting the culture. All samples were centrifuged at 6,000 × *g* for 7 min at 4°C. The supernatant fractions were decanted, and cell pellets were flash frozen in dry ice and ethanol and stored at −80°C until RNA extraction.

RNA was extracted using the RNeasy minikit from Qiagen, following the manufacturer's extraction protocol. A total of 3 μg of RNA was DNase treated using 2 units of Turbo DNase I enzyme (Invitrogen). A total of 1 μg of DNase-treated RNA was reverse transcribed using Superscript III reverse transcriptase (Invitrogen/Thermo Fisher). cDNA was amplified in an Applied Biosystems StepOne Plus Real-Time instrument using TaqMan MGB chemistry with primers and probes listed in Table S1. All reactions were performed in triplicate with four different cDNA concentrations (100, 50, 25, or 12.5 ng per reaction). Relative fold difference in transcript abundance was determined using the $\Delta\Delta C_T$ method of Pfaffl et al., with a PCR efficiency of >95% (45). Transcripts were normalized to *gyrB* abundance. At least 3 biological replicates were performed for each transcript. Results were statistically analyzed using a two-way ANOVA with Sidak's multiple-comparison test.

Metabolomics. UTI89, Δ*btsS*Δ*ypdB*, and Δ*sdaC* were grown in LB and incubated at 37°C with shaking, until cultures reached an OD_{600} = 0.5. Then, 1 M HCl was added to the culture to a final concentration of 10 mM (pH = 5). Cultures were incubated for another 15 min and then 1 mL of culture was collected. Cells were pelleted and supernatant was flash frozen and stored at −80°C until analyzed via Liquid Chromatography-Mass Spectrometry (LC-MS)-based metabolomics in the Vanderbilt Center for Innovative Technology (CIT). Isotopically labeled phenylalanine-D8 and biotin-D2 were added to 200 μL of culture supernatant per sample, and protein was precipitated by addition of 800 μL of ice-cold methanol followed by overnight incubation at −80°C. Precipitated proteins were pelleted by centrifugation (15,000 rpm, 15 min), and supernatants were dried down *in vacuo* and stored at −80°C. Individual samples were reconstituted in 120 μL of reconstitution buffer (acetonitrile/water, 90:10, vol/vol) containing tryptophan-D3, pyruvate-C13, valine-D8, and inosine-4N15. A quality control (QC) sample was prepared by pooling equal volumes from each individual sample. Quality control samples were used for column conditioning, retention time alignment and to assess mass spectrometry instrument reproducibility throughout the sample set and for individual batch acceptance.

LC-MS and LC-MS/MS analyses were performed on a high-resolution Q-Exactive HF hybrid quadrupole-Orbitrap mass spectrometer (Thermo Fisher Scientific, Bremen, Germany) equipped with a Vanquish UHPLC binary system and autosampler (Thermo Fisher Scientific, Germany). Metabolite extracts were separated on ACQUITY UPLC BEH Amide HILIC 1.7 μm, 2.1 × 100 mm column (Waters Corporation, Milford, MA) held at 30°C. Liquid chromatography was performed at a 200 μL min using solvent A (5 mM Ammonium formate in 90% water, 10% acetonitrile, and 0.1% formic acid) and solvent B (5 mM Ammonium formate in 90% acetonitrile, 10% water, and 0.1% formic acid) with a gradient length of 30 min.

Full MS analyses (6 μL injection volume) were acquired over 70 to 1,050 mass-to-charge ratio (*m/z*) in negative ion mode. Full mass scan was acquired at 120K resolution with a scan rate of 3.5 Hz, automatic gain control (AGC) target of 10e6, and maximum ion injection time of 100 ms. MS/MS spectra were collected at 15K resolution, AGC target of 2e5 ions, and maximum ion injection time of 100 ms.

The acquired raw data were imported, processed, normalized and reviewed using Progenesis QI v.3.0 (Non-linear Dynamics, Newcastle, UK). All MS and MS/MS sample runs were aligned against a QC (pooled) reference run. Unique ions (retention time and *m/z* pairs) were deadducted and deisotoped to generate unique "features" (retention time and *m/z* pairs). Data were normalized to all features using Progenesis QI.

Experimental data for measured serine (i.e., retention time and MS^2 fragmentation pattern) and pyruvate (i.e., retention time) was consistent with reference standards.

Pyruvate quantification. To collect samples for extracellular pyruvate quantification, strains were grown aerobically in LB to an OD_{600} = 0.5 and then split into two conditions: continued growth in LB alone, or in LB in which HCl was added to a final concentration of 10 mM. Samples were taken at time = 0, 15, 60, and 180 min after splitting the culture and normalized to an OD_{600} = 1.0. Samples were then centrifuged, and cell pellets and supernatant were separated, flash frozen, and stored at −80°C until assay was performed. Pyruvate Assay kits (MAK071-1KT, Sigma-Aldrich) were used to quantify pyruvate in the supernatant fraction according to the manufacturer's protocol. Fold change in pyruvate concentration was calculated by dividing the concentration of pyruvate in cells grown in acidic conditions over the concentration of pyruvate in cells grown in LB alone for each time point. Data were analyzed using 2-way ANOVA with a Dunnett's *post hoc* multiple-comparison test to compare the mutants to WT at each time point.

Statistical analysis. Statistical analyses were performed in GraphPad Prism, using the most appropriate test as indicated in the sections above and in the results. Details of sample size, test used, error bars, and statistical significance cutoffs are presented in the text or figure legends. All experiments were performed in at least three biological replicates. Representative graphs are shown for the luminescence

reporter assays. qPCR data were analyzed using 2-way ANOVA with a Sidak's multiple-comparison test to compare individual time points. LC-MS abundance values were plotted as ArcSinh normalized values.

Graphics. All graphical models and drawings were generated using BioRender.com.

SUPPLEMENTAL MATERIAL

Supplemental material is available online only.

DATA SET S1, XLSX file, 0.1 MB.
DATA SET S2, XLSX file, 18.7 MB.
DATA SET S3, XLSX file, 0.1 MB.
FIG S1, TIF file, 0.3 MB.
FIG S2, TIF file, 0.8 MB.
FIG S3, TIF file, 0.7 MB.
FIG S4, TIF file, 0.4 MB.
FIG S5, TIF file, 0.2 MB.
TABLE S1, DOCX file, 0.02 MB.
TABLE S2, DOCX file, 0.01 MB.

ACKNOWLEDGMENTS

We thank members of the Hadjifrangiskou and Schmitz labs for helpful discussions and critical reading of the manuscript. This work was supported by the National Institutes of Health under the following grants: P20DK123967 (M.H.), R01AI168468 (M.H.), T32 GM007569 (J.R.B.), and 2T32AI112541-06 (M.A.W.). This work was supported in part using the resources of the Center for Innovative Technology at Vanderbilt University.

M.A.W., B.D.S., and M.H. conceived the study, performed the experiments, analyzed the data, and composed the manuscript. A.B. and J.R.B. performed experiments, analyzed data, and edited the manuscript. A.C.S.-R., S.G.C., S.D.S., and J.A.M. optimized mass spectrometry methods, executed the metabolomics experiments, performed metabolomics data analysis, edited and reviewed the manuscript.

The authors have no conflicts of interest to declare.

REFERENCES

1. Lund P, Tramonti A, De Biase D. 2014. Coping with low pH: molecular strategies in neutralophilic bacteria. FEMS Microbiol Rev 38:1091–1125. https://doi.org/10.1111/1574-6976.12076.
2. Yamamoto S, Tsukamoto T, Fau- Terai A, Terai A, Fau- Kurazono H, Kurazono H, Fau- Takeda Y, Takeda Y, Fau- Yoshida O, Yoshida O. 1997. Genetic evidence supporting the fecal-perineal-urethral hypothesis in cystitis caused by Escherichia coli. J Urol 157:1127–1129. https://doi.org/10.1016/S0022-5347(01)65154-1.
3. Foster JW. 2004. Escherichia coli acid resistance: tales of an amateur acidophile. Nat Rev Microbiol 2:898–907. https://doi.org/10.1038/nrmicro1021.
4. Matsuzaki T, Scotcher D, Darwich AS, Galetin A, Rostami-Hodjegan A. 2019. Towards further verification of physiologically-based kidney models: predictability of the effects of urine-flow and urine-pH on renal clearance. J Pharmacol Exp Ther 368:157–168. https://doi.org/10.1124/jpet.118.251413.
5. Simerville JA, Maxted WC, Pahira JJ. 2005. Urinalysis: a comprehensive review. Am Fam Physician 71:1153–1162.
6. Price SB, Wright JC, DeGraves FJ, Castanie-Cornet M-P, Foster JW. 2004. Acid resistance systems required for survival of Escherichia coli O157:H7 in the bovine gastrointestinal tract and in apple cider are different. Appl Environ Microbiol 70:4792–4799. 15294816. https://doi.org/10.1128/AEM.70.8.4792-4799.2004.
7. Bergholz TM, Whittam TS. 2007. Variation in acid resistance among enterohaemorrhagic Escherichia coli in a simulated gastric environment. J Appl Microbiol 102:352–362. https://doi.org/10.1111/j.1365-2672.2006.03099.x.
8. Lin J, Lee IS, Frey J, Slonczewski JL, Foster JW. 1995. Comparative analysis of extreme acid survival in Salmonella typhimurium, Shigella flexneri, and Escherichia coli. J Bacteriol 177:4097–4104. https://doi.org/10.1128/jb.177.14.4097-4104.1995.
9. Lin J, Smith MP, Chapin KC, Baik HS, Bennett GN, Foster JW. 1996. Mechanisms of acid resistance in enterohemorrhagic Escherichia coli. Appl Environ Microbiol 62:3094–3100. https://doi.org/10.1128/aem.62.9.3094-3100.1996.
10. Kanjee U, Houry WA. Mechanisms of acid resistance in Escherichia coli.
11. Lu P, Ma D, Chen Y, Guo Y, Chen G-Q, Deng H, Shi Y. 2013. L-glutamine provides acid resistance for Escherichia coli through enzymatic release of ammonia. Cell Res 23:635–644. https://doi.org/10.1038/cr.2013.13.
12. De Biase D, Lund PA. 2015. The Escherichia coli acid stress response and its significance for pathogenesis, p 49–88. *In* Sariaslani S, Gadd GM (ed), Advances in Applied Microbiology, vol 92. Academic Press.
13. Pennacchietti E, D'Alonzo C, Freddi L, Occhialini A, De Biase D. 2018. The Glutaminase-dependent acid resistance system: qualitative and quantitative assays and analysis of its distribution in enteric bacteria. Front Microbiol 9:2869. https://doi.org/10.3389/fmicb.2018.02869.
14. Selvarasu S, Ow DS-W, Lee SY, Lee MM, Oh SK-W, Karimi IA, Lee D-Y. 2009. Characterizing Escherichia coli DH5α growth and metabolism in a complex medium using genome-scale flux analysis. Biotechnol Bioeng 102:923–934. https://doi.org/10.1002/bit.22119.
15. Cicchillo RM, Baker MA, Schnitzer EJ, Newman EB, Krebs C, Booker SJ. 2004. Escherichia coli L-serine deaminase requires a [4Fe-4S] cluster in catalysis. J Biol Chem 279:32418–32425. https://doi.org/10.1074/jbc.M404381200.
16. Zhang X, Newman E. 2008. Deficiency in l-serine deaminase results in abnormal growth and cell division of Escherichia coli K-12. Mol Microbiol 69:870–881. https://doi.org/10.1111/j.1365-2958.2008.06315.x.
17. Vining LC, Magasanik B. 1981. Serine utilization by Klebsiella aerogenes. J Bacteriol 146:647–655. https://doi.org/10.1128/jb.146.2.647-655.1981.
18. Chaussee MS, Somerville GA, Reitzer L, Musser JM. 2003. Rgg coordinates virulence factor synthesis and metabolism in Streptococcus pyogenes. J Bacteriol 185:6016–6024. https://doi.org/10.1128/JB.185.20.6016-6024.2003.
19. Foxman B. 2010. The epidemiology of urinary tract infection. Nat Rev Urol 7:653–660. https://doi.org/10.1038/nrurol.2010.190.
20. Mulvey MA, Schilling JD, Hultgren SJ. 2001. Establishment of a persistent Escherichia coli reservoir during the acute phase of a bladder infection. Infect Immun 69:4572–4579. https://doi.org/10.1128/IAI.69.7.4572-4579.2001.
21. Hannan TJ, Totsika M, Mansfield KJ, Moore KH, Schembri MA, Hultgren SJ. 2012. Host–pathogen checkpoints and population bottlenecks in persistent

and intracellular uropathogenic Escherichia coli bladder infection. FEMS Microbiol Rev 36:616–648. https://doi.org/10.1111/j.1574-6976.2012.00339.x.
22. Forde BM, Roberts LW, Phan M-D, Peters KM, Fleming BA, Russell CW, Lenherr SM, Myers JB, Barker AP, Fisher MA, Chong T-M, Yin W-F, Chan K-G, Schembri MA, Mulvey MA, Beatson SA. 2019. Population dynamics of an Escherichia coli ST131 lineage during recurrent urinary tract infection. Nat Commun 10:3643. https://doi.org/10.1038/s41467-019-11571-5.
23. Spaulding CN, Klein RD, Ruer S, Kau AL, Schreiber HL, Cusumano ZT, Dodson KW, Pinkner JS, Fremont DH, Janetka JW, Remaut H, Gordon JI, Hultgren SJ. 2017. Selective depletion of uropathogenic E. coli from the gut by a FimH antagonist. Nature 546:528–532. https://doi.org/10.1038/nature22972.
24. O'Hanlon DE, Come RA, Moench TR. 2019. Vaginal pH measured in vivo: lactobacilli determine pH and lactic acid concentration. BMC Microbiol 19:13. https://doi.org/10.1186/s12866-019-1388-8.
25. Mendling W. 2016. Vaginal microbiota, p 83–93. *In* Schwiertz A (ed), Microbiota of the human body: implications in health and disease. Springer International Publishing, Cham.
26. Kraxenberger T, Fried L, Behr S, Jung K. 2012. First insights into the unexplored two-component system YehU/YehT in Escherichia coli. J Bacteriol 194:4272–4284. https://doi.org/10.1128/JB.00409-12.
27. Steiner BD, Eberly AR, Hurst MN, Zhang EW, Green HD, Behr S, Jung K, Hadjifrangiskou M. 2018. Evidence of cross-regulation in two closely related pyruvate-sensing systems in uropathogenic Escherichia coli. J Membr Biol 251:65–74. https://doi.org/10.1007/s00232-018-0014-2.
28. Fried L, Behr S, Jung K. 2013. Identification of a target gene and activating stimulus for the YpdA/YpdB histidine kinase/response regulator system in Escherichia coli. J Bacteriol 195:807–815. https://doi.org/10.1128/JB.02051-12.
29. Kannan G, Wilks JC, Fitzgerald DM, Jones BD, BonDurant SS, Slonczewski JL. 2008. Rapid acid treatment of Escherichia coli: transcriptomic response and recovery. BMC Microbiol 8:37. https://doi.org/10.1186/1471-2180-8-37.
30. Chen SL, Hung C-S, Xu J, Reigstad CS, Magrini V, Sabo A, Blasiar D, Bieri T, Meyer RR, Ozersky P, Armstrong JR, Fulton RS, Latreille JP, Spieth J, Hooton TM, Mardis ER, Hultgren SJ, Gordon JI. 2006. Identification of genes subject to positive selection in uropathogenic strains of Escherichia coli: a comparative genomics approach. Proc Natl Acad Sci U S A 103:5977–5982. https://doi.org/10.1073/pnas.0600938103.
31. Gasperotti A, Göing S, Fajardo-Ruiz E, Forné I, Jung K. 2020. Function and regulation of the pyruvate transporter CstA in Escherichia coli. Int J Mol Sci 21:9068. https://doi.org/10.3390/ijms21239068.
32. Shin D, Lee E-J, Huang H, Groisman EA. 2006. A positive feedback loop promotes transcription surge that jump-starts salmonella virulence circuit. Science 314:1607–1609. https://doi.org/10.1126/science.1134930.
33. Behr S, Kristoficova I, Witting M, Breland EJ, Eberly AR, Sachs C, Schmitt-Kopplin P, Hadjifrangiskou M, Jung K. 2017. Identification of a high-affinity pyruvate receptor in Escherichia coli. Sci Rep 7:1388. https://doi.org/10.1038/s41598-017-01410-2.
34. Newman EB, Dumont D, Walker C. 1985. In vitro and in vivo activation of L-serine deaminase in Escherichia coli K-12. J Bacteriol 162:1270–1275. https://doi.org/10.1128/jb.162.3.1270-1275.1985.
35. Su H, Newman EB. 1991. A novel L-serine deaminase activity in Escherichia coli K-12. J Bacteriol 173:2473–2480. https://doi.org/10.1128/jb.173.8.2473-2480.1991.
36. Richard H, Foster JW. 2004. Escherichia coli glutamate- and arginine-dependent acid resistance systems increase internal ph and reverse transmembrane potential. J Bacteriol 186:6032–6041. https://doi.org/10.1128/JB.186.18.6032-6041.2004.
37. Maurer LM, Yohannes E, Bondurant SS, Radmacher M, Slonczewski JL. 2005. pH Regulates genes for flagellar motility, catabolism, and oxidative stress in Escherichia coli K-12. J Bacteriol 187:304–319. https://doi.org/10.1128/JB.187.1.304-319.2005.
38. Zhang X, El-Hajj Ziad W, Newman E. 2010. Deficiency in l-serine deaminase interferes with one-carbon metabolism and cell wall synthesis in Escherichia coli K-12. J Bacteriol 192:5515–5525. https://doi.org/10.1128/JB.00748-10.
39. Shao Z, Newman EB. 1993. Sequencing and characterization of the sdaB gene from Escherichia coli K-12. Eur J Biochem 212:777–784. https://doi.org/10.1111/j.1432-1033.1993.tb17718.x.
40. Takahashi N, Saito K, Schachtele CF, Yamada T. 1997. Acid tolerance and acid-neutralizing activity of Porphyromonas gingivalis, Prevotella intermedia and Fusobacterium nucleatum. Oral Microbiol Immunol 12:323–328. https://doi.org/10.1111/j.1399-302x.1997.tb00733.x.
41. Scott DR, Marcus EA, Weeks DL, Sachs G. 2002. Mechanisms of acid resistance due to the urease system of Helicobacter pylori. Gastroenterology 123:187–195. https://doi.org/10.1053/gast.2002.34218.
42. Justice SS, Hunstad DA, Seed PC, Hultgren SJ. 2006. Filamentation by Escherichia coli subverts innate defenses during urinary tract infection. Proc Natl Acad Sci U S A 103:19884–19889. https://doi.org/10.1073/pnas.0606329104.
43. Persson K, Petersson U, Johansson C, Demirel I, Kruse R. 2022. Transcriptional alterations in bladder epithelial cells in response to infection with different morphological states of uropathogenic Escherichia coli. Sci Rep 12:486. https://doi.org/10.1038/s41598-021-04396-0.
44. Murphy KC, Campellone KG. 2003. Lambda Red-mediated recombinogenic engineering of enterohemorrhagic and enteropathogenic E. coli. BMC Mol Biol 4:2002–2007. https://doi.org/10.1186/1471-2199-4-11.
45. Pfaffl MW. 2001. A new mathematical model for relative quantification in real-time RT-PCR. Nucleic Acids Res 29:e45. https://doi.org/10.1093/nar/29.9.e45.